

# Probing Viscoelasticity of a Coiled Flagella System

Claire Atkinson

*2024 Physics REU, University of California, Santa Barbara*

*Department of Physics, University of Washington*

Nicholas L. Cuccia (Graduate Advisor) and Zvonimir Dogic (Faculty Advisor)

*Department of Physics, University of California, Santa Barbara*

(Dated: September 30, 2024)

A material’s ability to flow depends heavily upon the thermal motion of its constituent particles, but quantitatively making this connection remains challenging. We explore this relationship through a model colloidal system consisting of bacterial flagella, a micron-sized, helical biological filament. Point mutations of the flagella’s protein structure create various discrete shapes, which allows for control of the degree to which filaments intertwine and entangle. By imaging the diffusion dynamics of the system, we determine how such geometric entanglements between particles slow thermal motion, making the overall solution more resistant to flow. To quantify the length and time of flagellar diffusion, we take measurements of the mean squared displacement. Here, we focus on coiled flagella, the most flexible and tightly-wound helix. Microscopically, we observe that shorter coils form arcs that undergo an effective one-dimensional random walk about the center of the coil. Longer coils, on the other hand, are almost entirely caged on all time scales. This produces a material on the macroscopic level that behaves as a physical gel, which indicates that the flow dynamics of a system are dictated by its most confined element. Understanding the connection between the microscopic and macroscopic regime allows for the design of exotic materials where one has precise control over emerging flow properties.

## I. INTRODUCTION

Many everyday items exhibit unique flow properties. Toothpaste, for instance, holds its shape on short timescales while deforming over long periods of time [1, 2]. This behavior arises because toothpaste is a complex fluid that consists of a combination of polymer and solvent [3]. The underlying solvent has a fluid-like response, whereas the entangled polymers imbue elasticity [4, 5]. The microscopic polymers exhibit thermal motion that causes them to diffuse through the system. However, diffusive motion is constrained in unique ways depending on the geometry of the underlying polymers and how they intertwine [6]. The filaments are effectively caged by their neighbors, which constrains their motion and gives rise to timescale-dependent properties on the large-scale [7]. Polymers are typically flexible filaments and have an ill-defined shape, making it difficult to describe their entanglements [8]. We quantify the effect of filament geometry on entanglements and resultant bulk flow properties using a biological filament whose shape is well-defined and tunable: bacterial flagella.

Flagella are a rigid protein filament used by bacteria for locomotion [9]. Once isolated from the bacterial body, these naturally helical molecules behave as elastic springs on the microscopic scale [10]. Due to the nature of its flagellin subunits, flagella can assume eleven unique conformational states [9, 11]. This allows us to study the impact of filament shape on large-scale material properties. For example, a dense suspension of straight rods is less resistant to flow than an otherwise identical solution prepared with helical rods [12]. The helical flagella interdigitate with one another, which restricts their motion; in

order to linearly translate, the helices must also rotate, resulting in an effective corkscrewing motion. Straight rods, whose geometry does not couple rotation to translation, diffuse over much shorter timescales. Therefore, the flagella system provides a mechanism for geometric control of the microscopic motion, which in turn determines the macroscopic viscoelasticity of a suspension.

The dynamics of helical, straight, and combination copolymer flagella systems have been studied, including their microscopic diffusion and bulk viscoelasticity [12]. We focus on flagella whose shape is “coiled” [10]. The helical nature of this molecule imbues the overall structure with flexibility despite the filament’s underlying stiffness. Since coiled flagella have the tightest pitch ( $\sim 0.5 \mu\text{m}$ ) and largest outer diameter ( $1.0 \mu\text{m}$ ) of any conformation [9], it has been shown to be the most flexible conformation, emulating the behavior of a slinky [10].

Here, we observe how this underlying flexibility couples to the rheological softness of the dense suspension in comparison to a similar suspension containing normal flagella. Additionally, the paper outlines how the longest and most confined filaments in the system bestow and determine its properties as a highly-entangled network.

## II. METHODS

Flagella were grown and isolated using a modified version of the protocol laid out previously [13–15]. To isolate a salmonella colony, we streaked 2% agarose plates with the coiled mutant EM9708. A single colony was placed into 50 mL of Luria-Bertani (LB) media and grown at  $37^\circ\text{C}$  while being shaken at 250 RPM until reaching an

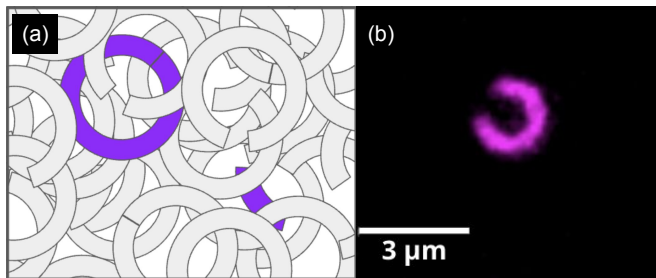


FIG. 1. A dense suspension of short coiled flagella (a) depicted as a cartoon and (b) imaged using confocal microscopy. The purple filaments are those that have been labeled fluorescently

OD600 around 1. The small-scale growth was diluted with LB by a factor of 10,000. 550  $\mu$ L of the diluted stock was added to 550 mL of LB media, which was subsequently grown at 37  $^{\circ}$ C and 150 RPM for 12 hours. The final OD600 of the large-scale growth was between 3 and 4.

To pellet the bacteria, the suspensions were spun down for 1 hour at 5000G and 4  $^{\circ}$ C. The pellets were resuspended using 50 mL of a buffer of 10 mM phosphate (pH 7.0) and 150 mM NaCl. Once homogenized, the solution was pushed through a 20G needle, shearing the flagella off of the bacterial bodies. The bacterial cell bodies were separated from the flagella via differential centrifugation: The suspension was centrifuged at 5000G for 30 minutes, pelleting the bacterial bodies while leaving the flagella in the supernatant. The supernatant was then transferred to a clean tube. This procedure was repeated until there was a thin white film at the edge of the pellet, indicating that all bacteria had been pelleted.

To pellet the flagella, we spun at 10,000 RPM for 4 to 5 hours, resulting in a well-defined grayish pellet. These pellets were resuspended in a buffer consisting of 10 mM potassium phosphate (pH 7.0) and 0.01% w/v Tween-20. The surfactant was included to discourage sticking and aggregation amongst the flagella.

The concentration of a flagella suspension was determined using a spectrophotometer (Thermo Scientific NanoDrop One): a flagella suspension was heated at 65  $^{\circ}$ C for 10 minutes to denature the protein, and its concentration was determined by measuring the absorbance at 280 nm. Denatured samples showed a clear peak at 280 nm, and the protein concentration was estimated using the extinction coefficient  $E(1\%, 280\text{ nm}) = 3.6$  [16].

Flagella can be labeled with amine-reactive dye due to their exposed amino groups [12]. We placed 1 mg/mL flagella into phosphate buffer (pH 8.0) and added an amine-reactive rhodamine [5-(and-6)-Carboxytetramethylrhodamine-succinimidyl ester, Fisher Scientific] to achieve a molar-fold excess of 10. This mixture was incubated at room temperature for an hour before excess dye was removed through dialysis. The labeling efficiency was calculated using a spectrophotometer calibrated to the flagellin monomer and the dye used.

For our experiments, we utilized dense suspensions containing labeled and unlabeled flagella. Specifically, the suspension consisted of labeled flagella ( $\frac{1}{10000}$  mg/mL), unlabeled flagella (4 mg/mL), Trolox (5 mM), sucrose (25 mM), potassium phosphate buffer (10 mM), and Tween-20 (0.01 % w/v). The sucrose was added as a stabilizing agent to suppress a conformation change observed in labelled flagella. Trolox prevented rapid photobleaching. Once made, the suspension was placed in a water bath at 25  $^{\circ}$ C for at least two hours to allow it to equilibrate. Following this procedure, all flagella were observed to be in the coiled state.

This sample was then placed into a parafilm chamber roughly 100 microns thick and sealed with UV glue. These labeled coiled flagella were imaged using 561-nm wavelength light on a spinning disk confocal microscope over varied time and z-dimension. We used a 100x oil-type objective with variable numerical aperture to adjust to the index of refraction of the sucrose. There were two distinct rates of data acquisition. For motions over hours, 50-ms exposure time was used with 1-s intervals. To observe more immediate motions, data were acquired at 50-ms exposure with 100-ms delay.

A Python package (pyImageJ) was used to process the images. First, a background subtraction was performed, followed by a Gaussian blur. Finally, the images were thresholded to remove excess noise. All images were taken of coils that were in-plane to best facilitate analysis, meaning that the circular cross-section of the helix was showing. A circle-fitting package in Python (circle-fit) enabled the tracking of filament motions over time. Coil rotations were quantified based on the difference in location between a coil's center of mass and the center of the fitted circle. Mean squared displacement data was then extracted using a tracking package (trackpy).

To analyze the bulk flow properties, we placed samples in a rheometer (AR-G2) utilizing a conical geometry (40 mm diameter, 2  $^{\circ}$  angle, and 55  $\mu$ m truncation gap). The sides of the cone were sealed with mineral oil to prevent evaporation of the sample. The measurements were taken at 25  $^{\circ}$ C without any preshear.

### III. RESULTS

When probing material properties, we examine how the shape and flexibility of the coiled flagella impact the response of the overall suspension to deformation.

#### A. Microscopic Dynamics

When taking data, the flagella are separated into groups by contour length to probe whether they diffuse distinctly. The “arcs” are those helices that do not reach one full pitch, and the “full coils” are longer than or equal to one full pitch. Upon observation, arcs diffuse

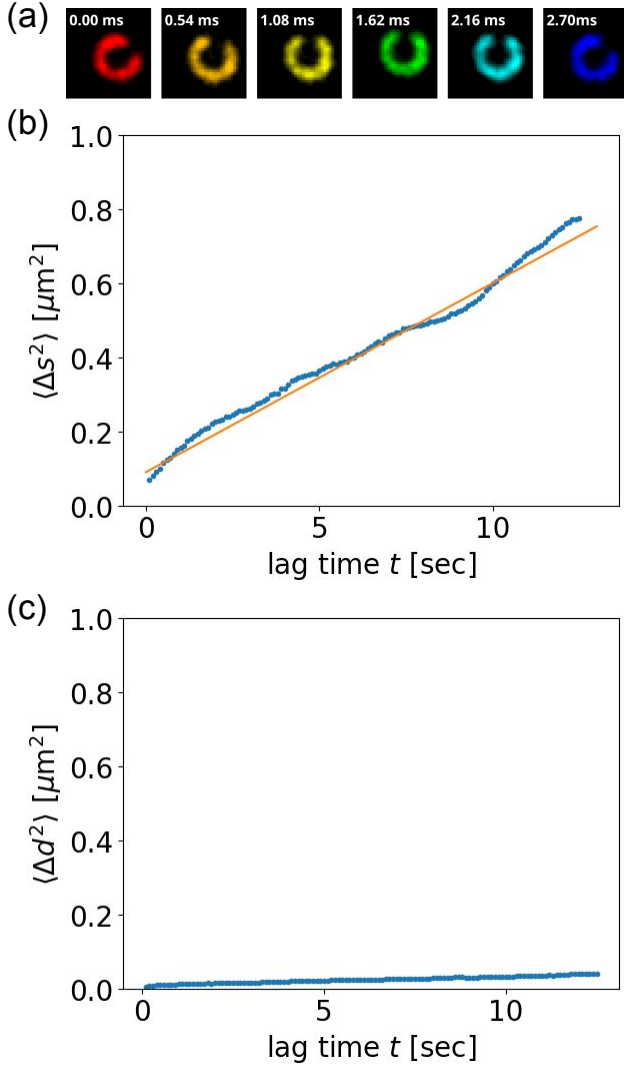


FIG. 2. Short timescale modes of diffusion for incomplete coils, referred to here as “arcs” (a) An arc rotates about its center point, which stays relatively confined (b) It experiences the analog of a one-dimensional random walk when rotating about its center with diffusion constant  $D = 0.026 \mu\text{m}^2/\text{s}$  (c) The center point of an arc is heavily constrained in diffusion

faster and reorient more often than their full coil counterparts. The full coils stay heavily confined on all observed timescales and rarely reorient. This creates an interesting dichotomous system to be examined, as depicted in Figure 1a.

The shortest arcs entangle the least, making them difficult to image since they do not remain in one plane long enough to extract meaningful data. As such, the majority of data comes from longer arcs, typically nearing the length of one coil, as shown in Figure 1b. As will be shown, the rheology of the system is dictated by its longer, most heavily entangled filaments; hence, focusing analysis on longer filaments still provides a representative description of the microscopic behavior.

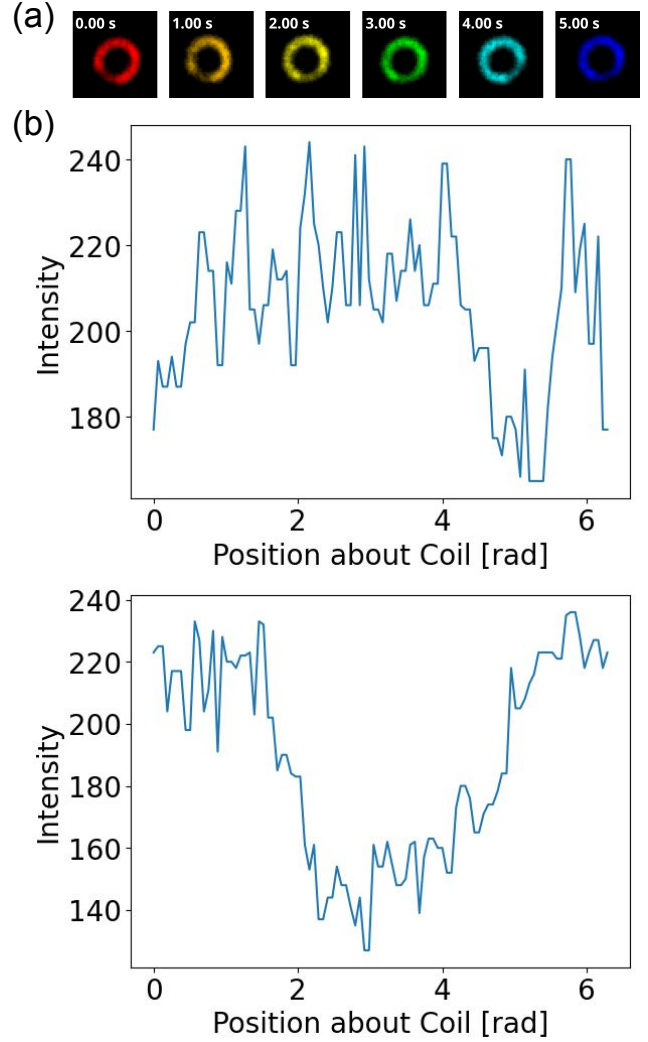


FIG. 3. Assessment of the contrast in intensity between the first and second coils of the same helix (a) There is a clear low point in intensity in images of the full coils where it can be inferred that the filament completes one full turn about its helical axis. By tracking this point, the rotation of a full coil can be analyzed (b) The drop in brightness over a segment of the coil can be quantified using the intensity values coded into the image. The graphs shown here depict a decrease in the intensity values over a portion of the same coil at 0 and 500 seconds respectively

We first examine the diffusive dynamics of the arcs. Over short periods of time ( $\sim 10$  seconds) they rotate about their center point – defined as the long axis through the center of the helix – while the center point itself remains stationary, which Figure 2a illustrates qualitatively. This is reflected quantitatively in the mean squared displacement data. The analysis of rotational displacement (Figure 2b) follows a linear trend, which indicates that this motion is entirely random. In this way, we can conceptualize arc motion about its center as a random one-dimensional walk. The diffusion constant

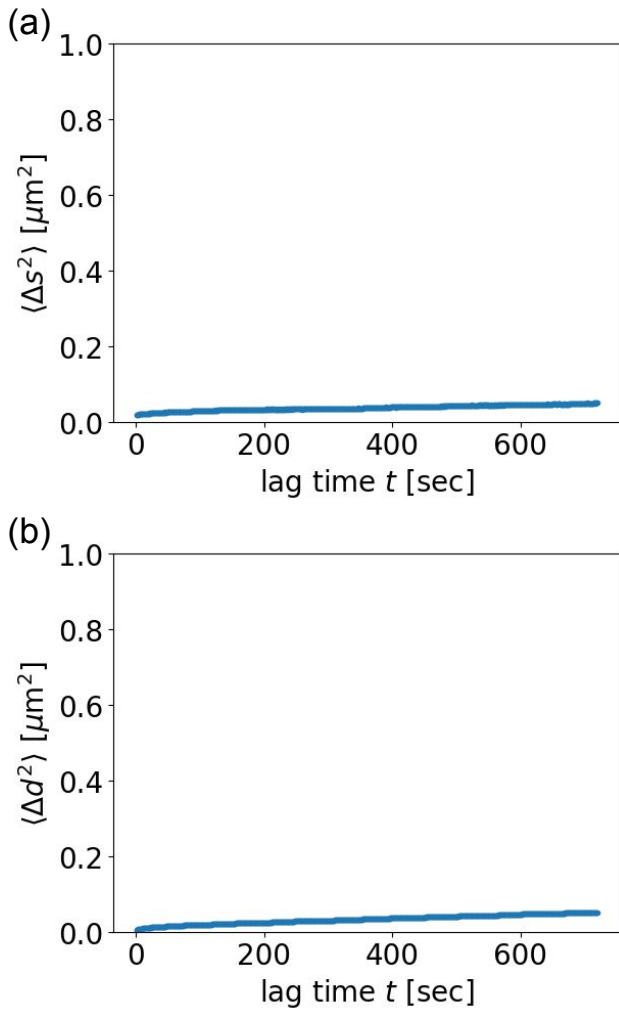


FIG. 4. Diffusive dynamics for coils longer than one pitch – known as “full coils” – on longer timescales (a) A full coil is constrained in its rotation about its center point (b) A full coil is constrained in its center-of-mass translation

describing the speed at which the flagella diffuse by rotation within the solution is  $D = 0.026 \mu\text{m}^2/\text{s}$ . Over these same short periods of time, the arc’s center point is confined since any drift observed on that timescale is within the noise of the microscope (Figure 2c). On longer timescales of about a minute, we qualitatively observe that their center of mass reorients, and the arc repeats this same behavior in a new plane.

The full coils can be analyzed similarly in terms of their center of mass translation and rotation about their long axis. Figure 3a depicts the motion of a single full coil over five seconds. Despite the fact that these in-plane coils form full circles in the field of view, we can still quantify their rotation. To do this, we take advantage of the intensity differences along the coil that can be observed in Figure 3a and is quantified in Figure 3b. Since it appears consistently, we infer this dip in brightness to be the point at which the coil wraps back around itself.

In contrast to the arcs, full coils move less than a micron on the order of hours. Both rotation and translation are constrained, as can be observed qualitatively in Figure 3a. Over the five seconds depicted, the center of the coil does not exhibit any significant displacement. The coil’s rotation also appears to be limited since the location of the dim segment has only slight variation that takes place over seconds as opposed to the millisecond rotations of the arcs. These dynamics are quantified in the mean squared displacement graphs shown in Figure 4. Since there is no linear trend and all variation is within the microscope’s resolution limit, the graphs support the idea that the coils are caged in both rotation and center of mass translation on both second- and minute-long timescales.

## B. Macroscopic Properties

To quantify the macroscopic behavior of a dense suspension of coiled flagella, we turn to rheological analysis, the result of which is depicted in Figure 5a. A dense suspension of coiled flagella exhibits viscoelasticity since the storage and loss moduli are both consistently nonzero. The storage modulus is larger than the viscous modulus for all frequencies, indicating a predominantly solid response. This response is analogous to that of a physical gel.

We compare this data to the rheological analysis of a dense suspension of normal flagella at a concentration of 7 mg/mL, shown in Figure 5b. The higher concentration of normal flagella accounts for the higher viscosity of the sucrose used in the coiled flagella suspension. The systems respond similarly under rheology: Both exhibit viscoelasticity with an elastic response that is predominantly stronger than the viscous response. A crossover between the elastic and viscous response occurs at high frequencies. However, this is likely a result of the machine’s inertia rather than the response of the material.

Interestingly, the magnitude of the response of the coiled flagella is weaker than that of the normal flagella by an order of magnitude. As such, the coiled suspension is softer than the normal suspension.

## IV. DISCUSSION

The data supports the idea that coils longer than one pitch are confined on all relevant time scales. Coils shorter than one pitch also undergo limited motion of their center of mass on short timescales, but on longer timescales they reorient into distinct planes. Further, they diffuse freely in rotation about their center of mass on both short and long timescales. The shortest arcs experience almost no caging and are able to diffuse freely in both rotation and center-of-mass translation over all observable lengths of time. The gel-like strain response

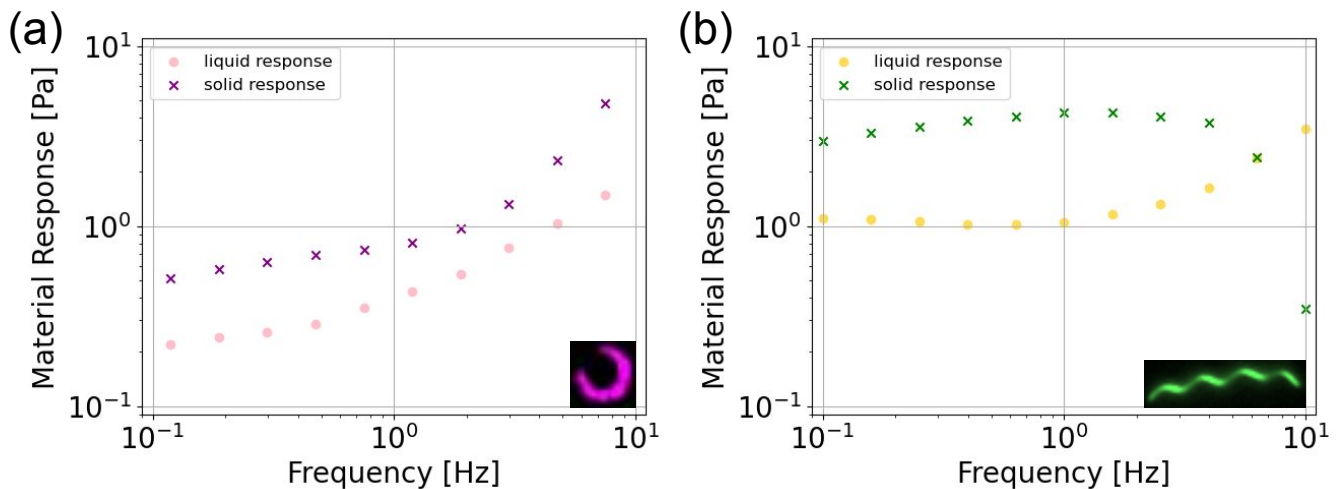


FIG. 5. Measurements of the bulk flow properties of (a) a dense suspension of coiled flagella and (b) a dense suspension of normal flagella

of the material is thereby most heavily influenced by the system's most heavily-confined filaments, the full coils.

The softness of the coiled dense suspension, in comparison, is more elusive in its connection to the microscopic regime. It is likely that the flexibility of the coils results in this lower-magnitude material response. Even in confinement, this element of flexibility allows for additional recoil of the system that could account for the lower-magnitude strain response.

More data should be taken to illuminate diffusive modes on different time scales to further probe this interesting system. For the full coils, imaging over shorter intervals would allow for the resolution of any minuscule vibrations made by the filaments. Taking longer videos of arcs would allow for the analysis of reorientation events on longer timescales. Both of these measurements would be indicative of the cage size of the respective molecules. Additionally, it would be beneficial to find a way to image very short arcs so that the mean squared displacement analysis conducted would be more representative

of the entire arc population. Lastly, the strain response magnitude of various coiled systems could be analyzed to determine whether coil flexibility is the true cause of this material's softness.

## ACKNOWLEDGMENTS

This work is supported by NSF REU grant PHY-2349677. I would like to thank my faculty advisor, Professor Zvonimir Dogic, and my graduate mentor, Nicholas L. Cuccia, for their gracious support, mentorship, and guidance throughout this project. Additionally, I greatly appreciate the welcoming and supportive atmosphere created by those in the flagella group and the Dogic Lab as a whole. Their efforts have made my time at UCSB truly illuminating and enjoyable. Lastly, a huge thanks to program director Sathya Guruswamy for making this whole experience possible.

- 
- [1] E. Vranić, A. Lacević, A. Mehmedagić, and A. Uzunović, Formulation ingredients for toothpastes and mouthwashes, *Bosnian journal of basic medical sciences* **4**, 51–58 (2004).
  - [2] A. Becker, F. Katzen, A. Pühler, and L. Ielpi, Xanthan gum biosynthesis and application: a biochemical/genetic perspective, *Appl. Microbiol. Biotechnol.* **50**, 145–152 (1998).
  - [3] R. H. Ewoldt and C. Saengow, Designing complex fluids, *Annu. Rev. Fluid Mech.* **54**, 413 (2022).
  - [4] M. Kröger, Simple models for complex nonequilibrium fluids, *Physics Reports* **390**, 453 (2004).
  - [5] N. L. Cuccia, S. Pothinenia, B. Wua, J. M. Harpera, and J. C. Burton, Pore-size dependence and slow relaxation of hydrogelfriction on smooth surfaces, *Proc. Natl. Acad. Sci.* **117**, 11247–11256 (2020).
  - [6] T. T. Perkins, D. E. Smith, and S. Chu, Direct observation of tube-like motion of a single polymer chain, *Science* **5160**, 819 (1994).
  - [7] J. Käs, H. Strey, and E. Sackmann, Direct imaging of reptation for semiflexible actin filaments, *Nature* **368**, 226 (1994).
  - [8] M. Rubinstein and R. H. Colby, *Polymer Physics* (Oxford University Press, 2003) Chap. 1, p. 38.
  - [9] S.-I. Aizawa, *Molecular Medical Microbiology*, 2nd ed., edited by Y.-W. Tang, M. Sussman, D. Liu, I. Poxton, and J. Schwartzman (Academic Press, 2015) Chap. 7 - Flagella, pp. 125–146.

- [10] N. C. Darnton and H. C. Berg, Force-extension measurements on bacterial flagella: triggering polymorphic transformations, *Biophysical journal* **92**, 2230–2236 (2007).
- [11] S. V. Srigiriraju and T. R. Powers, Continuum model for polymorphism of bacterial flagella, *Phys. Rev. Lett.* **94**, 248101 (2005).
- [12] S. Yardimci, T. Gibaud, W. Schwenger, M. R. Sartucci, P. D. Olmsted, J. S. Urbach, and Z. Dogic, Bonded straight and helical flagellar filaments form ultra-low-density glasses, *Proc. Natl. Acad. Sci.* **120** (2023).
- [13] S. Yardimci, *Networks formed by rigid filaments of tunable shape*, Ph.D. thesis, Brandeis University (2014).
- [14] S. Asakura, G. Eguchi, and T. Iino, Reconstitution of bacterial flagella in vitro, *J. Mol. Biol.* **10**, 42 (1964).
- [15] S. Asakura and T. Iino, Polymorphisms of salmonella flagella as investigated by means of in-vitro copolymerization of flagellins derived from various strains, *J. Mol. Biol.* **64**, 251 (1972).
- [16] F. V. et al., Terminal region of flagellin are disordered in solution, *J. Mol. Biol.* **209**, 127–133 (1989).